Mine Water Environ (2016) 35:64–76
DOI 10.1007/s10230-015-0347-3

TECHNICAL ARTICLE

Mixing of Acid Rock Drainage with Alkaline Ash Leachates: Formation of Solid Precipitates and pH-Buffering

Lotta Sartz[1,2] · Mattias Bäckström[2] · Stefan Karlsson[2] · Bert Allard[2]

Received: 3 October 2014 / Accepted: 9 May 2015 / Published online: 20 May 2015

Abstract Three metal-rich, acidic mine waters (from Bersbo and Ljusnarsberg, Sweden) were mixed with alkaline fly ash leachates in various proportions, representing a pH titration. Changes in pH and the loss of metals in solution due to precipitation of solid phases were tracked. Mineral equilibria and changes in pH and alkalinity were simulated using the geochemical code PHREEQC and the MINTEQv4 database, and the measured and simulated pH responses were compared. The formation of solid precipitates corresponded to fairly well-defined pH-buffering regions, reflecting the mine water compositions (notably the levels of Fe, Al, and Mn). Zn precipitation had a distinct buffering effect at near-neutral pH for the mine waters not dominated by iron. The formation of solid Mg phases (carbonate, as well as hydroxide) was indicated at high pH (above 9), but not formation of solid Ca phases, despite high sulfate levels. The phases that precipitated were various amorphous mixtures, mostly of the metals Fe, Al, Mn, Zn, and Mg. For the Fe-rich mine water, pH was poorly simulated with a simple MIX model, while alkalinity predictions agreed reasonably well with measured data. For the Al-rich mine waters, the simulated pH responses agreed well with the measurements. In an additional step, geochemical simulations were performed where selected proxy phases for major elements were forced to precipitate; this significantly improved the pH and alkalinity predictions. This approach may be more efficient than performing mixing experiments and titrations.

Keywords ARD · CFB-fly ash · PHREEQC

Introduction

Historic sulfidic mine waste dumps generally contain coarse-grained, highly-weathered material (Lefebvre et al. 2001). Continued sulfide oxidation generates acid rock drainage (ARD) that leaches substantial quantities of elements (e.g. Cu, Zn, Cd, Pb, As, and Fe). Precipitation and accumulation of metals in river banks, stream sediments, lake shores, etc. are common downstream of such areas (Bowell and Parshley 2005; España et al. 2006; Herbert Jr. 2006; Moncur et al. 2006; Schroth and Parnell Jr. 2005; Varesel and Gomes 2009). Secondary phases of Fe, Al, and Mn, along with other adsorbed and co-precipitated contaminants, serve as potential new contaminant sources (Baresel et al. 2006; Bowell and Parshley 2005; Shum and Lavkulich 1999a, b).

Alkaline materials, including waste products like incineration residues (e.g. fly ash), have been used to neutralize acid-generating mine waste as well as ARD (Gitari et al. 2006, 2008; Mackie and Walsh 2012; Pérez-López et al. 2007a, b; Polat et al. 2002; Xenidis et al. 2002). Fly ash (FA) was also used in a trace element immobilization study by Bäckström and Sartz (2011), who showed that common cationic ARD elements (like Cu, Pb, and Zn) are effectively immobilized through precipitation and sorption, with an increased pH. However, FA often contains high concentrations of other potentially toxic

Electronic supplementary material The online version of this article (doi:10.1007/s10230-015-0347-3) contains supplementary material, which is available to authorized users.

✉ Lotta Sartz
lotta.sartz@oru.se

[1] Bergskraft Bergslagen AB, Harald Olsgatan 1, 714 31 Kopparberg, Sweden

[2] Man-Technology-Environment Research Centre, Örebro University, 701 82 Örebro, Sweden

elements, such as Cr, Mo, and Ba. Bäckström and Sartz (2011) found that Mo leaching could be kept at a low level if the pH was kept below 7 and that leaching of the more toxic Cr(VI) could be avoided in the presence of ferrous iron, as Cr(VI) was reduced to Cr(III) and precipitated/co-precipitated as a hydroxide at a pH > 4. In addition, FA may contain organic contaminants (Johansson 2003), which also must be considered before full-scale applications are performed.

When solid alkaline materials are acting as neutralizing agents for mine waste or ARD, there is a risk for clogging and passivation of the neutralizing minerals. Nevertheless, alkaline amendments have proven to be effective in a lot of field studies, e.g.: Bersbo historic copper mines, Sweden (Bäckström et al. 2009; Karlsson and Bäckström 2003), the Butte, MT, USA mining district (Davis et al. 1999), the Heath Steele mine site, New Brunswick, Canada (Yanful et al. 1993), oxic limestone drains (Cravotta III and Trahan 1999), and permeable apatite barriers, Coeur d'Alene mining district, USA (Conca and Wright 2006).

Neutralization of ARD and metal immobilization by addition of alkaline solutions is another option. This includes active treatment, with an alkaline solution added to an ARD effluent (Cravotta III et al. 2010), and more passive treatment methods, e.g. leach beds (Kruse et al. 2012). Simmons et al. (2002) suggested that alkaline steel slag could be placed in a leach bed, producing an alkaline leachate that neutralized the ARD in a mixing zone. This method is advantageous for well-defined iron-rich ARD discharges since clogging and passivation of reactive surfaces in filters and barriers can be avoided. Prediction of gained pH depending on the dosing of alkali and the actual mine water is very important (Cravotta III et al. 2010) as is proper prediction of alkalinity generated as the two leachates mix, because this determines how resistant the approach is to pH fluctuations.

The hydrolysis of cations consumes alkalinity with a buffering effect in a pH region determined by the corresponding thermodynamic complex formation constant, c.f. Eq. 1 (Pillay et al. 2001).

$$M(H_2O)_n^{z+} \leftrightarrow \{M(H_2O)_{n-1}(OH)\}^{(z-1)+} + H^+ \quad (1)$$

Surface complex formation (adsorption) of cations by solid hydrous oxides also releases protons from the surfaces, further buffering the pH, as shown in Eqs. 2, 3, and 4 (Schindler and Stumm 1987).

$$S - OH + M^{z+} \leftrightarrow S - OM^{(z-1)+} + H^+ \quad (2)$$

$$2S - OH + M^{z+} \leftrightarrow (S - O)_2 M^{(z-2)+} + 2H^+ \quad (3)$$

$$S - OH + M^{z+} + H_2O \leftrightarrow S - OMOH^{(z-2)+} + 2H^+ \quad (4)$$

The formation of solid metal hydroxides (or carbonates) in supersaturated systems has the largest pH-regulating and buffering effect. Titration of ARD containing dissolved Fe and Al with a strong base would be expected to exhibit two inflection points in the titration curve (pH vs amount of added base), corresponding to Fe(III) hydrolysis at a pH $\approx$ 2.7 and Al at a pH $\approx$ 4.5, respectively, followed by precipitation of Fe in the pH interval 2.8-4.5 (formation of schwertmannite, followed by ferrihydrite) and a basaluminite-like Al-hydroxysulphate mineral at pH 4–5 (España et al. 2006; Lee et al. 2002). These Fe and Al phases serve as excellent scavengers of other hydrolyzable metals in the system. Mn hydroxides generally precipitate at a pH > 7, which make them less important as trace metal scavengers in ARD (Bigham et al. 1996; España et al. 2006; Lee et al. 2002). Precipitation of Cu and Zn at pH 5.0–6.5 and 6.5–7.5, respectively, is also of great importance as pH buffering processes (Liu and Kalin 1992; Totsche et al. 2006). Totsche et al. (2003) used a combination of experimental titration, PHREEQC modeling, and mineralogical analysis (IR-spectroscopy and X-ray diffraction) to assess relevant pH buffering mechanisms in a highly acidic mine lake. Their mineralogical analyses indicated the formation of poorly crystalline schwertmannite as well as various Al hydroxides and hydroxy sulfates.

We analyzed the formation of solid precipitates and successive pH changes when mixing acidic, metal-rich mine waters from field sites with alkaline FA leachates. Various solid phases dominate in different pH regions, reflecting the proportions of precipitating and co-precipitating metals (Fe, Al, Mn, Zn, and Mg). Mineral equilibria and changes of pH and alkalinity were measured as well as simulated with the geochemical modeling program PHREEQC and the MINTEQv4 database (Parkhurst and Appelo 1999). The aims of our study were to: (1) elucidate the pH-controlling buffering processes and their effect on the distribution and mobility of dissolved metals in real systems (depending on the constituents of the mine water); (2) compare buffering between measured and modeled systems, especially prediction of pH and alkalinity, and; (3) see if modeled predictions (of pH and alkalinity) can be easily improved. The fate and immobilization of trace elements from both the mine waters and the ash water have been reported in an earlier paper (Bäckström and Sartz 2011).

Materials and Methods

Mine Waters and Ash Leachates

Mine waters were selected so as to have one that was Fe dominated (BO), one that was Al dominated (LB), and one that contained more Mn (LG). Acidic mine waters were sampled at two historic sulfidic ore mining sites: (1) the

Bersbo (BO) mine discharge, Östergötland (N58.26495°, E16.03165°) (Allard et al. 1987), and (2) the Bondstollen (LB) shaft, and (3) the Gustaf (LG) shaft, both at the Ljusnarsberg mine, Bergslagen (N59.87805°, E14.98816°) (Bäckström and Sädbom 2008). The Ljusnarsberg mine field was discovered in 1624 and was last mined in 1975 (Bäckström and Sädbom 2008). The source of the economic mineralisation has been complex mixtures of chalcopyrite ($CuFeS_2$). sphalerite (ZnS), galena (PbS), pyrrhotite (FeS), pyrite (FeS_2), and magnetite (Fe_3O_4), without carbonates or skarn minerals. Until the late nineteenth century, mining was mainly focused on the Cu and secondary Fe ore. The Cu ore was dominated by disseminated chalcopyrite ($CuFeS_2$) that occurs as small lenses and veinlets. The chalcopyrite is more or less mixed with pyrrhotite, pyrite, and magnetite. From the middle of the nineteenth century and onwards, galena and sphalerite ore was also produced.

Copper mining at the Bersbo site had already begun by the 14th century (Tegengren 1924). The ore was estimated as 0.5–3 % Cu; 1–3 % Zn; 1 % Pb, 20 % Fe, and approximately 25 % sulphur (Allard et al. 1987; Karlsson and Bäckström 2003). Mining left about 1 million m^3 of waste rock, which contains a complex mixture of sulphides (pyrite, chalcopyrite, sphaelerite, and galena) in a matrix of amphibolitic intrusions in leptite.

The dissolved organic carbon (DOC) in the outlet from the Bersbo mine deposit area is generally ≤2 mg/L, representing humic and fulvic acid of low average molecular weight originating from the groundwater (Pettersson et al. 1993). Contributions from surface waters are minor; the deposit area was covered with clay after remediation in 1988–1990. Concentrations of DOC are somewhat higher at the Ljusnarsberg site, indicating a greater contribution of shallow groundwater, but are still ≤5 mg/L.

FA was sampled from a circulating fluidized bed (CFB) boiler (using wood and peat fuel) at an incineration plant for district heating in the region (operated by E.ON). The ash was leached with water (10 L/s) for 24 h. Despite high levels of carbon in the ash, only a minor fraction was released by leaching with water, giving DOC levels generally below 10 mg/L (for 5–10 L/s). According to Pavasars et al. (1997), 10–15 % of the DOC should be hydrophilic acids, 45–55 % other hydrophilic agents, with the rest being hydrophobic compounds. The hydrophilic acid fraction is dominated by low molecular weight aliphatic carboxylic acids.

In an earlier project (Bäckström and Karlsson 2006), ash from the same boiler was analysed for polycyclic aromatic hydrocarbon (PAH) content and dioxin and dioxin-like compounds toxicity (CELCAD and DR CALUX). The total PAH content was found to be very low at 0.14 mg/kg. No carcinogenic PAH was identified in the sample. A total dioxin and dioxin-like toxicity of 56 pg/g biotoxic equivalents was found. This is low compared to other ashes (Johansson 2003).

Mixing of Mine Waters and Ash Leachates

Mine waters and ash leachates were mixed in Sarstedt tubes (50 mL) in proportions ranging from 1 to 20 % ash leachate for LB and LG, and 1–50 % leachate for BO (Table 1). 25 mixtures were assessed for each mine water. The tubes were shaken on an end-over-end shaker for 7 days and then allowed to settle for 24 h prior to sampling of the overlying water phase.

Chemical Analysis

Samples were filtered through 0.40 µm polycarbonate filters and analyzed for pH, electrical conductivity (Radiometer CDM 210), alkalinity, and inorganic anions. Alkalinity was determined from end-point titration (0.02 M HCl) to pH 5.4 during nitrogen purging of the solution using an ABU93 Triburette connected to a TIM900 Titration Manager (Radiometer). An endpoint of pH 5.4 is the

Table 1 Fraction (%) of ash leachates in the mine water–ash leachate mixes

Mix no	% Ash leachate		
	BO	LG	LB
1	0.0	0.0	0.0
2	1.0	1.0	1.0
3	2.0	2.0	2.0
4	3.0	3.0	3.0
5	4.0	4.0	4.0
6	5.0	5.0	5.0
7	6.0	5.5	5.5
8	7.0	6.0	6.0
9	8.0	6.5	6.5
10	9.0	7.0	7.0
11	10.0	7.5	7.5
12	11.0	8.0	8.0
13	12.0	8.5	8.5
14	13.0	9.0	9.0
15	14.0	9.5	9.5
16	15.0	10.0	10.0
17	16.0	10.5	10.5
18	17.0	11.0	11.0
19	18.0	11.5	11.5
20	19.0	12.0	12.0
21	20.0	13.0	13.0
22	22.0	14.0	14.0
23	25.0	15.0	15.0
24	30.0	17.0	17.0
25	50.0	20.0	20.0

Swedish standard for titrimetric determination of carbonate alkalinity (Swedish Standards Institute 2002). Chloride and sulfate were determined by capillary zone electrophoresis (CZE) using an Agilent ^{3D}CE system. The carrier electrolyte was a 5 mM chromate buffer (pH 8) with 0.5 mM tetradecyltrimethylammonium bromide (TTAB) (Jones and Jandik 1991; Romano et al. 1991). Injection was done hydrostatically at 10 mbar for 30 s. Samples were preserved with nitric acid (1 %) prior to elemental analysis by ICP-MS (Agilent 4500). The internal standard was ^{103}Rh, and the analytical quality was ascertained by frequent analysis of standards.

Geochemical Calculations: Measured Data

Chemical speciation was calculated from the measured concentrations in solution for each of the 25 mixtures of mine water/ash leachate (1–25 for BO, LG, and LB, respectively), using the geochemical code PHREEQC (version 2.15.0; Parkhurst and Appelo 1990) with the MINTEQ.v4 database. The solubility of schwertmannite (Yu et al. 1999) was added to the data base, and the contribution to the alkalinity from Al species was adjusted to be compatible with the before-mentioned end-point titration standard (pH 5.4 compared to pH 4.5). The pe used in the geochemical calculations were calculated from measured redox potentials from an earlier study using the same reactants ($pe = 0.059 \times Eh$ (V)). A strong correlation ($r^2 = 0.86$) was found between pe and pH ($pe = -0.6 \times pH + 4.2$) (Sartz 2010). Redox potentials were in agreement with those suggested by Baas-Becking et al. (1960), Church et al. (2007), and Valiente et al. (1991) and were in the pe-region 9–12 for the mine waters and −1 for ash waters. Expected solid phases were assessed, as well as saturation indices (SIs). SI is defined as the ratio between the ion activity product and the solubility constant. A positive SI (>0.5) indicates supersaturation, a negative SI (<0.5) indicates under-saturation, and an SI in the range of −0.5 to 0.5 is considered to represent equilibrium with the specific solid phase.

Geochemical Simulations

MIX Only

PHREEQC simulations were performed using the MIX keyword to simulate a titration corresponding to mixing the two solutions, mine water and ash leachate, at the same ratios as in the experiments. MIX keyword calculates conservative concentrations based on the concentrations in solution of the two end-members, according to Eq. 5, which assesses a conservative initial concentration, after mixing but prior to any reactions:

Table 2 Composition of the fresh mine waters from Bersbo outlet (BO), Ljusnarsberg, Gustaf (LG) and Ljusnarsberg, Bondstollen (LB) and the corresponding ash leachates (10 L/s) used in the mixing experiments

	Mine waters			Ash leachates	
	LB	LG	BO	LB, LG	BO
pH	5.0 (5.2)	5.0 (4.3)	3.3 (3.1)	12.3	12.6
El. cond. (μS/cm)	1000	1100	1400	9500	9700
Acidity (meq/l)	0.2	0.3	4.9	0	0
Alkalinity (meq/l)	0	0	0	33	43
DOC[a](mg/ l)	<5	<5	<2	<10	<10
Cl^- (mg/l)	<1	<1	20	220	240
SO_4^{2-} (mg/l)	560	650	680	1300	1600
Na (mg/l)	9.2	8.4	9.3	63	51
K (mg/l)	5.3	5.0	18	430	540
Mg (mg/l)	36	42	20	<0.001	0.03
Ca (mg/l)	150	200	81	1400	1000
Fe (mg/l)	0.9 (0.9)	12 (0.8)	100 (80)	0.28	0.01
Mn (mg/l)	2.7	4.5	5.6	<0.001	0.005
Al (mg/l)	20	12	4.1	<0.001	0.030
Rb (μg/l)	25	25	30	1900	2300
Sr (μg/l)	92	160	430	3600	3600
Ba (μg/l)	91	87	120	290	360
Cr (μg/l)	<1	<1	<1	270	200
Co (μg/l)	34	35	200	0.8	<0.5
Ni (μg/l)	5.9	7.1	22	12	6.7
Cu (μg/l)	5000	600	1600	3	10
Zn (μg/l)	26,000	16,000	43,000	80	110
Mo (μg/l)	<0.5	<0.5	<0.5	590	590
Cd (μg/l)	50	20	80	<1	<1
Pb (μg/l)	350	40	40	40	70

Iron concentrations and pH after 1 week are given within parentheses

[a] Estimated maximum levels assessed from previous analyses of waters from the sites and of representative leachates

$$X_{mine\ water} \times C_{mine\ water} + X_{ash\ leachate} \times C_{ash\ leachate} \quad (5)$$

for each component in solution, where X is the fraction of mine water and ash leachate in each mix (Table 1) and C is the concentration of the component in the original end member solutions (Table 2).

MIX Including Solids

The MIX simulation was modified in an attempt to get a more accurate prediction of alkalinity and gained pH. As discussed in the introduction, various solid phases dominate in different pH regions and the metals of concern are the major elements responsible for buffering reactions: Fe, Al, Mn, Mg, and Zn. One representative solid phase, denoted as a "proxy phase", was chosen for each of the major

elements, based on the results of the geochemical calculations using the measured data. The SI for the proxy phases were decreased by 0.5 SI units compared to the MIX-only simulation by defining them with EQUILIBRIUM_PHASES in the input file for PHREEQC. This action tells the program that the degree of supersaturation should be lowered, thus removing dissolved species from the solution (i.e. forcing the solid phase to precipitate). Thus, 25 simulated mixes were made for BO, LG, and LB. The geochemical simulations were performed in two steps: (1) the end-members were mixed at the same ratios as in the experiment, and (2) buffering was simulated by the precipitation of selected solid phases. The two steps are referred to as "MIX only" and "MIX including solids", respectively

Results and Discussion

Major Elements

Data for the mine waters and ash leachates are given in Table 2. Ca, Mg, and sulfate levels were high in all three mine waters. The Bersbo mine water (BO) was particularly rich in iron as well as zinc and the Ljusnarsberg waters (LB and LG) were rich in Al. Ca, K, and Na were high in the ash leachates, as were levels of Cr, Mo, Sr, Rb, and Ba (although low in the mine waters).

The mixing of ARD with alkaline ash water leads to a gradual increased pH. However, the pH is also affected by the formation of metal hydroxides and carbonates, giving inflection points to the pH curve. The major elements (Fe, Al, Mn, Mg, and Zn) in the mine waters all precipitated with increasing proportions of alkaline ash leachate (Figs. 1, 2). The precipitates and co-precipitates were amorphous and ill-defined. The colors of the precipitates are shown in Fig. 1 and in the supplemental figures that accompany the on-line version of this paper. They go from orange-yellow to dark orange in system BO, from orange-yellow to dark brown in system LG, and from colorless/white to dark brown in system LB. These colors can be helpful in discussions of precipitated phases. For example, Shum and Lavkulich (1999a) used color as a surrogate variable to estimate extractable Fe content in mine waste rock.

Fe and Al were both removed from solution at pH 4.5 and above in the BO system. Fe precipitated at a lower pH than Al and was by far the predominant precipitate in this system. Fe and Al followed a similar trend in the LG system, but Fe was quantitatively precipitated from the start, at pH 4, while Al was not quantitatively precipitated until a pH of at least 6.5. The Fe level was low in the LB system, which was dominated by white Al precipitates up to a pH of 8.5.

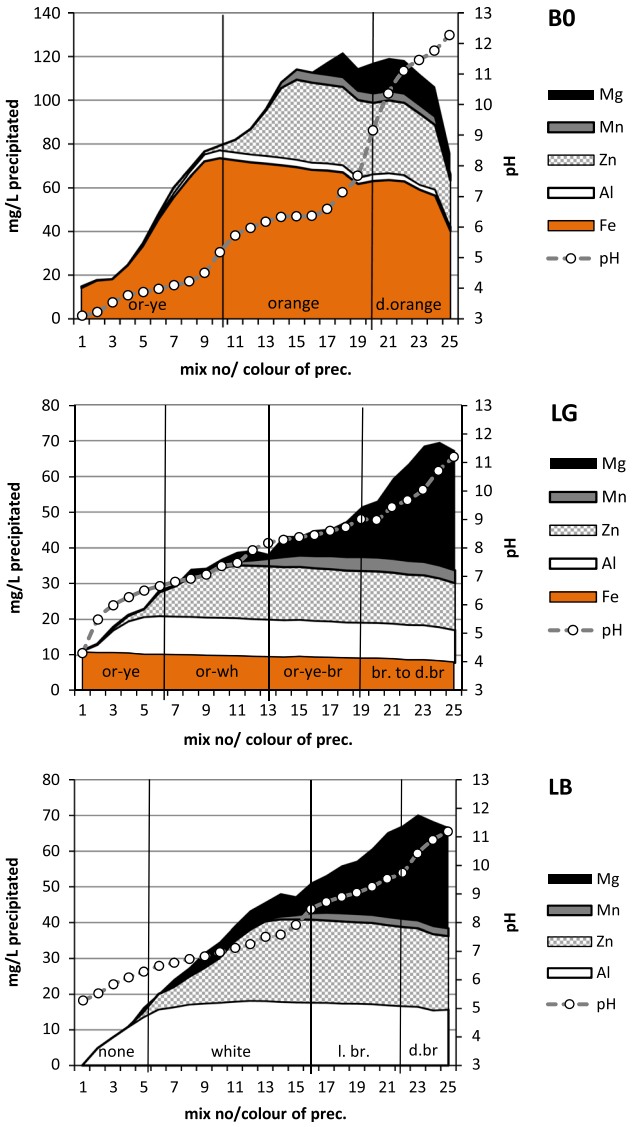

Fig. 1 Precipitated/sorbed amounts of major elements (in mg/L), pH and colour of precipitate. Color codes are: *orange-yellow* (or-ye), *orange* (orange), *dark orange* (d.orange), *orange-white* (or-wh), *orange-yellow–brown* (or-ye-br), *brown to dark brown* (br. to d.br), no color (none), *white* (white) and *light brown* (l.br.)

Mn precipitated at a lower pH in the BO system (fully precipitated at pH 6.5) than in the LB and LG systems, where a pH of almost 9 was required for quantitative removal. Zn was removed, probably by a combination of sorption, precipitation, and coprecipitation, at a pH of 5.5–6.5 for the BO system and almost a pH unit higher for the LB and LG systems. Trace element behavior was reported in Bäckström and Sartz (2011).

Mg started to precipitate at pH 6.5 in the BO system, but was not quantitatively precipitated until pH 11. In the LB and LG system, Mg precipitation started at pH 9, and was quantitative at a pH of 10.5–11 and above. Ca, Na, and K remained dissolved in all of the systems.

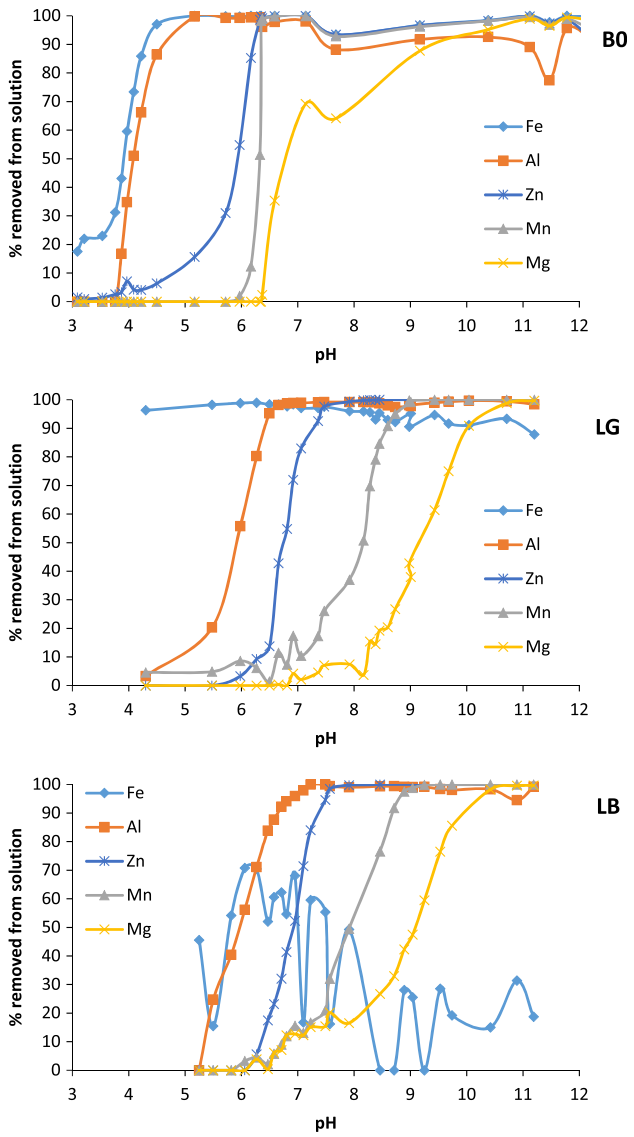

Fig. 2 Metal removal (%) from solution as a function of pH

Precipitated Species

The Iron-Rich BO System

Fe entirely dominated precipitation up to a pH of ≈4.5 (mixture 9) and is the major constituent at higher pHs. The color of the precipitate was yellow-orange in mixtures 1–9, orange/orange-brown in 10–18, and dark orange in 19–25 (Fig. 1). The mineralogical composition of the Fe phase in the fresh precipitate was assumed to be amorphous and ill-defined (Totsche et al. 2003), and was therefore not analyzed with XRD. PHREEQC calculations indicate supersaturation with respect to schwertmannite ($Fe_8O_8(OH)_6SO_4$), goethite, and ferrihydrite over the entire pH region. Schwertmannite or a mixture of schwertmannite and goethite were probably the dominant Fe phases below pH 4.5 (Bigham et al. 1996; Burgos et al. 2012; España et al. 2006; Zhu et al. 2012), while the principal phase above 4.5 would probably be ferrihydrite or goethite (Burgos et al. 2012). Varesel and Gomes (2009) identified a mixture of schwertmannite and goethite in the pH 2.5–3.8 region in the yellow-orange Fe-rich precipitate downstream of a similar mine waste deposit in Portugal, and further downstream (at higher pH), the precipitate was dominated by goethite (orange to brown). Thus, the pH buffering that corresponds to the plateau in the pH curve at a pH around 3–4.5 predominantly reflects schwertmannite precipitation (Eq. 6; Totsche et al. 2003).

$$16Fe^{3+} + xSO_4^{2-} + (68 - 2x)H_2O \leftrightarrow Fe_{16}O_{16}(OH)_{16-2x}(SO_4)_x(s) + 36H_2O + (48 - 2x)H^+ \quad (6)$$

The plateau observed for mixtures 10–17 correlates with Al precipitation, which starts at a pH of ≈4 (mixture 5). PHREEQC calculations indicate that alunite ($KAl_3(SO_4)_2(OH)_6$) may precipitate at pH 4–5 and above. Precipitation of various Al-hydroxysulfates (basaluminite, alunite) in ARD at pHs ≥ 4.5 has previously been suggested (Burgos et al. 2012; España et al. 2006; Lee et al. 2002; Totsche et al. 2003). Amorphous aluminum hydroxide may precipitate at pHs of 5–10 (mixtures 10–20), which correlates with the pH plateau ≈5.5–7 and the corresponding pH buffering, in agreement with the neutralization experiments with Burra Burra Creek water reported by Lee et al. (2002).

Removal of Zn from solution is observed at pH 5 and above. There is, however, no evident Zn phase that can be expected to precipitate except the carbonate smithsonite ($ZnCO_3$) at pH 8–10, and the hydroxide at higher pH. Zinc removal at pH < 8 may be due to coprecipitation with Fe (and Al) and/or adsorption on these phases. The slight increase in solubility at pH > 8 (Fig. 2) may reflect desorption and/or formation of soluble hydroxides e.g. $Zn(OH)_3^-$ (Baes and Mesmer 1976). Zinc is not considered to contribute to the pH buffering to any appreciable extent in this system due to the dominance of Fe.

The carbonates, rhodochrosite ($MnCO_3$) and magnesite ($MgCO_3$), were close to equilibrium at pH above 7.5 (mixtures 19–25), whereas pyrochroite ($Mn(OH)_2$) and brucite ($Mg(OH)_2$) were saturated at pH 10 and above. This agrees with the observed precipitation of brucite at a pH of 10.5 (Leentvaar and Rebhun 1982). Manganite (MnOOH) was supersaturated in mixtures 20–25 (pH above 9). Thus, Mn would be solubility controlled by rhodochrosite at pH 7–9 and by manganite and pyrochroite at higher pH, and Mg would be solubility controlled by magnesite at pH 7–10 and by brucite at pH above 10. Although precipitation of rhodochrosite and magnesite theoretically would be expected to buffer pH and decrease alkalinity, no distinct

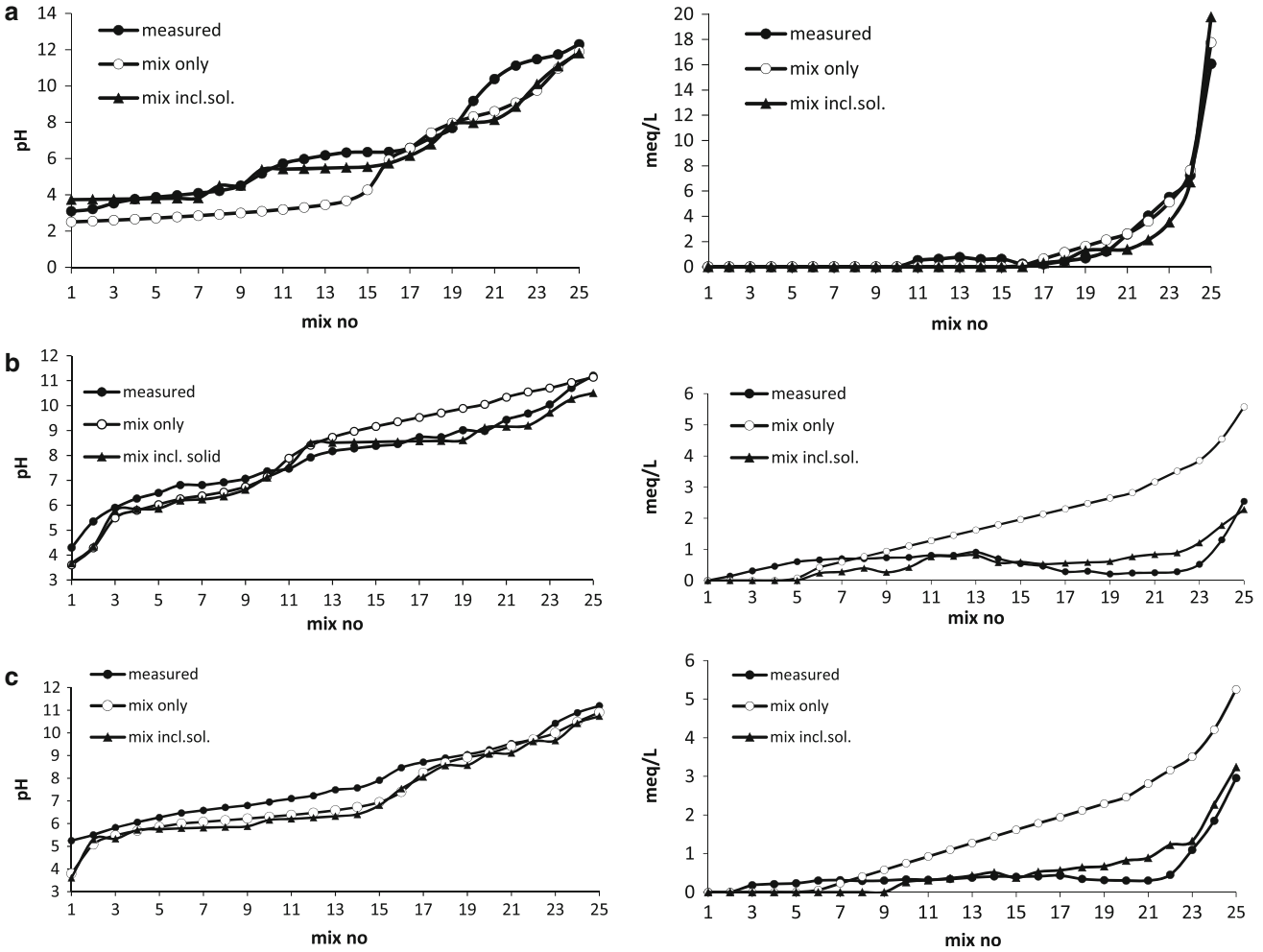

Fig. 3 **a** Measured and modelled (*MIX only* and *MIX including solids*) pH and alkalinity in the BO system. **b** Measured and modelled (*MIX only* and *MIX including solids*) pH and alkalinity in the LG system. **c** Measured and modelled (*MIX only* and *MIX including solids*) pH and alkalinity in the LB system

plateau was observed at pH > 7. Instead, both pH and alkalinity increased rapidly at pH > 7 (Fig. 3a). However, neither Mn nor Mg were dominant elements in this system, and the precipitation of these phases had no significant pH buffering effect.

LG System: Iron and Aluminum-Rich System

Iron is quantitatively removed from solution in the entire pH range of 4–11 (Fig. 2). Based on the PHREEQC calculations, which suggest supersaturation of ferrihydrite in all mixes, Fe is assumed to precipitate as a hydrous ferric oxide. At mixture 6 (pH 6.5), the color of the precipitates changes from orange to orange-white, corresponding to the removal of Al from solution. Saturation indices for both alunite and gibbsite in the pH region 6.5–7.5 (mixtures 6–12) indicate equilibrium and the precipitation of these phases would consequently contribute to the observed pH buffering with a plateau between pH 6 and 7.5. Gibbsite is close to saturation or supersaturation in the mixtures 13–25 (pH above 7.5), and hence, gibbsite is probably the solubility limiting Al phase at high pH.

Zinc may precipitate as smithsonite at pH 6.5–7.5, which also seems to contribute to the buffer plateau between mixtures 6–11. PHREEQC calculations indicate undersaturation at pHs > 7.5 (mixtures 13–25). Thus, the quantitative removal of dissolved Zn at pH above 7.5 reflects sorption, as well as coprecipitation with Fe and Al. An additional explanation for the removal of Zn at high pH could be the formation of the mixed Mn-Zn phase chalcophanite ($ZnMn_3O_7{\cdot}3H_2O$). The incorporation of Zn in chalcophanite was recently studied by Hayes et al. (2009), Korshin et al. (2007) and Kwon et al. (2009). Uptake of Zn by various manganese oxides has also been observed (Adams et al. 2009). This may explain the quantitative removal of Mn from solution at pH > 7.5.

Table 3 Potentially solubility controlling phases and pH regions of precipitation

Name	Formula	pH-region	References
Schwertmannite	$Fe_8O_8(OH)_6SO_4$	2.8–4.5	Bigham et al. (1996), Lee et al. (2002), Wu et al. (2009)
Ferrihydrite	$Fe(OH)_3 \times nH_2O$	>4	Lee et al. (2002), Wu et al. (2009)
Goethite	FeOOH	>4.5[a]	Lee et al. (2002), Wu et al. (2009)
Alunite	$KAl_3(SO_4)_2(OH)_6$	4–6	Nordstrom (1982), Shum and Lavkulich (1999b)
Gibbsite	$Al(OH)_3$	>6	Nordstrom (1982)
$Zn(OH)_2$	$Zn(OH)_2$	6.5–7.5	Liu and Kalin (1992), Sayilgan et al. 2010)
Rhodochrosite	$MnCO_3$	7–9	Present study
Magnesite	$MgCO_3$	7–9.5	Present study
Smithsonite	$ZnCO_3$	6.5–8.5	Present study
Manganite	MnO(OH)	>7	Lee et al. (2002), España et al. (2006)
Brucite	$Mg(OH)_2$	>10.5	Leentvaar and Rebhun (1982)

[a] Not directly from acid mine waters

Both rhodochrosite and magnesite reach equilibrium at pH 8–9 (mixtures 13–20), and a distinct color change was noticed between mixtures 12 and 13 (from orange-white to orange-brown). Magnesite precipitation may explain the drop in alkalinity observed for mixtures 13–20 (Fig. 3b). Magnesite was undersaturated in mixture 21, corresponding to a rapid increase in both pH and alkalinity, and the solubility of Mg at pH > 10 was most likely controlled by brucite, which would be expected to precipitate in mixtures 21–25. Rhodochrosite was undersaturated ≥pH 9, but manganite (MnOOH) was close to equilibrium and could be the solubility-limiting phase at the high pH of mixture 13 (≥pH 7.5), in agreement with previous observations (España et al. 2006).

LB System: Aluminum-Rich System

Fe levels were low, and there was no pH buffering effect from Fe precipitating in the LB system. Al dominated the precipitate at low pH (5–6.5), as Zn and Mg did at higher pHs. PHREEQC calculations indicate supersaturation with respect to alunite and gibbsite from mixtures 1–11 (pH 5–7). Above pH 7, alunite becomes undersaturated, whereas gibbsite is at equilibrium. The white precipitate at pH 5–6 is darker and more brownish with increasing pH.

Precipitation of smithsonite at pH 6–7 is assumed, while undersaturation is indicated with respect to smithsonite as well as zinc hydroxide at pH > 7. Still, Zn is almost quantitatively removed from solution from pH ≥ 7, indicating sorption and/or coprecipitation with Al. Sorption/incorporation into hydrous manganese oxides is also a reasonable explanation for Zn removal, as assumed for the LG system.

Rhodochrosite and magnesite are likely to be at equilibrium in mixtures 12–19 (pH 7.5–9) and 17–21 (8.5–9.5), respectively. The low alkalinity (Fig. 3c) of these solutions (mixtures 12–21) could be due to the precipitation of carbonates removing carbonate from solution. At high pH (>10), Mn is probably solubility controlled by manganite (at equilibrium in mixtures 20–25) and Mg by brucite (at equilibrium in mixtures 23-25).

Geochemical Simulations

Some potentially solubility limiting solid phases are listed in Table 3. Based on the observed and/or assessed precipitated phases, the following phases were chosen as proxy phases for the major elements: Fe—ferrihydrite ($Fe(OH)_3$), Al—gibbsite ($Al(OH)_3$), Zn—amorphous $Zn(OH)_2$, Mn—manganite (MnOOH), and Mg—brucite ($Mg(OH)_2$). These proxy phases align with Cravotta III et al. (2010), who assumed that the metals precipitated as $Fe(OH)_3$, $Al(OH)_3$, $Mn(OH)_2$, and $Mg(OH)_2$ for Fe, Al, Mn, and Mg, respectively. Geochemical simulations were performed in two steps: (1) the end-members were mixed at the same ratios as in the experiment, i.e. simulation of conservative mixing ("MIX only"), and (2) buffering was simulated through precipitation of selected solid phases ("MIX including solids"). By decreasing the SI from the "*MIX only*" calculations, the proxy phases were forced to precipitate. Calculated SIs for the selected proxy phases are given in Fig. 4a–c.

BO System: Iron-Rich System

The shapes of the SI curves (measured and "MIX only", respectively) are in fair agreement for all of the selected proxy phases (Fig. 4a). However, the SI for "MIX only" is below the measured SI for all systems at low pH (mixtures 1–15), which reflects the corresponding predicted pH, which was lower than the measured pH (Fig. 3a). Gibbsite, in particular, was calculated to be undersaturated until mixture 16 in "MIX only". However, Al is removed from

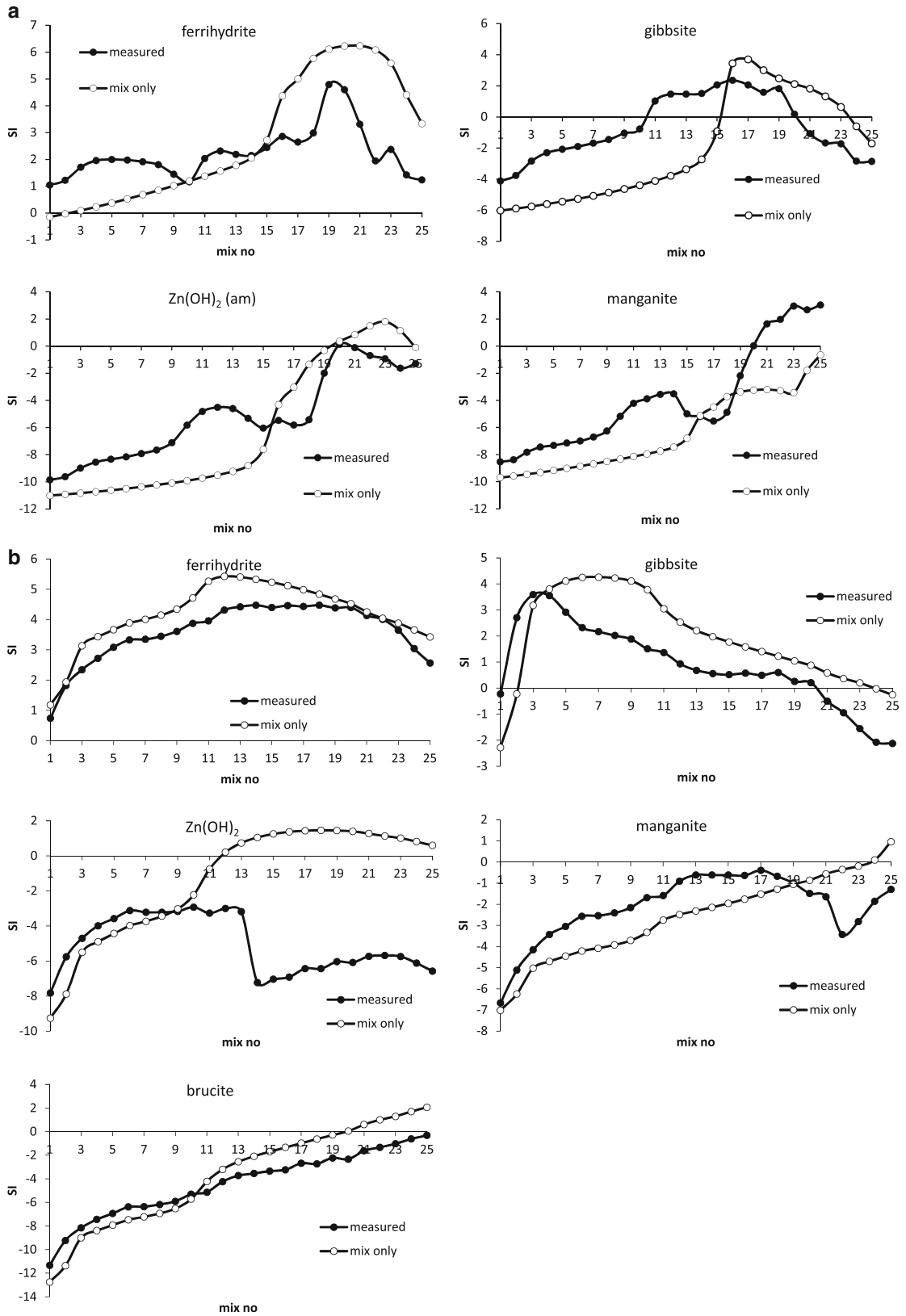

Fig. 4 **a** Measured and modelled (*MIX only*) saturation indices for selected minerals in the BO system. **b** Measured and modelled (*MIX only*) saturation indices for selected minerals in the LG system. **c** Measured and modelled (*MIX only*) saturation indices for selected minerals in the LB system

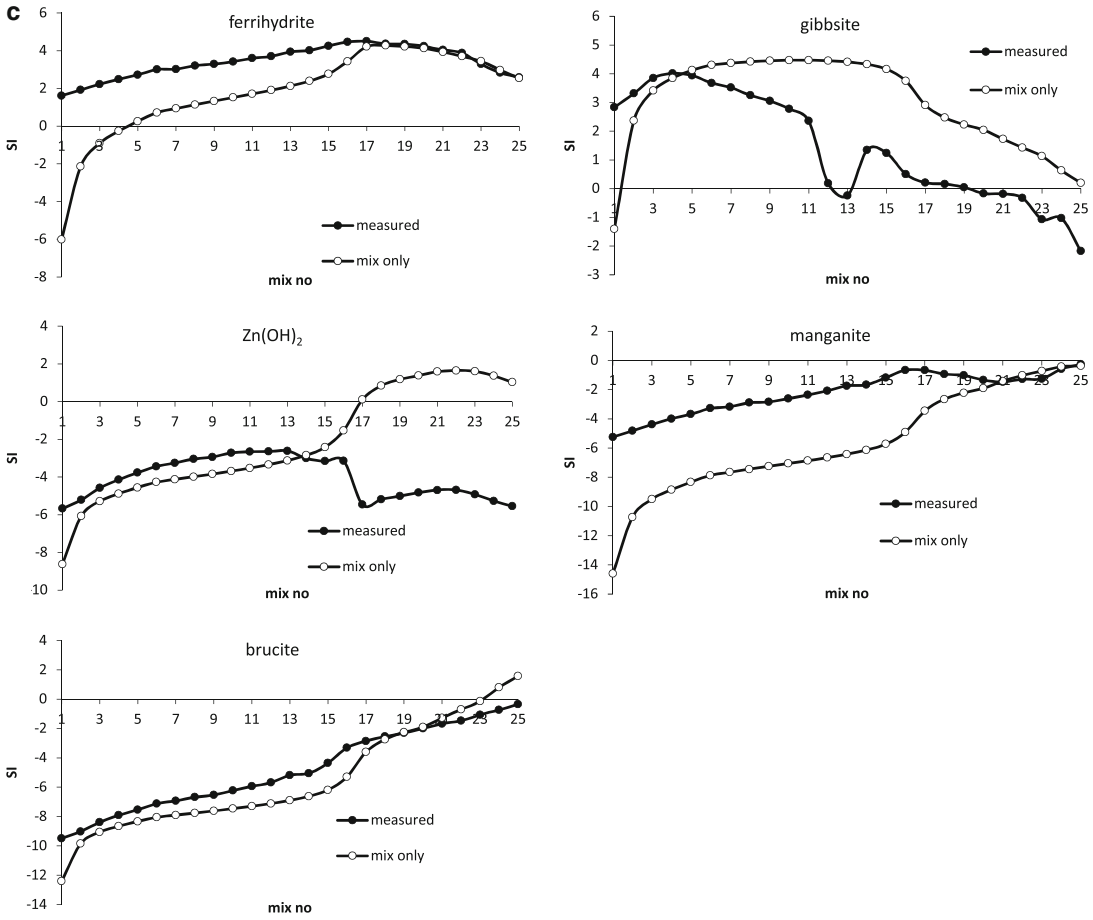

Fig. 4 continued

solution at pH ≈ 5, and hence Al precipitation would take place in mixes where net acidity was <0. At a pH ≈ 5, the change between acidity to alkalinity is mainly a matter of the H^+/OH^- balance (contribution from carbonates are negligible) and would hence correspond rather well to conservative calculations for the two end-members. From the conservative calculations (Eq. 5), it was found that the net acidity would be <0. Consequently, the "MIX including solids" was adjusted for supersaturation of gibbsite. The SI value of "MIX only" at mixture 16 was chosen, which led to a better prediction of pH (Fig. 3a). This operation forced the system to assume a higher Al concentration than is possible based on the two end-members. However, the theoretical calculation only considered one solid phase, while Table 3 also indicates the formation of alunite at low pH, which could explain the difference between measured and "MIX only".

LG System: Iron and Aluminum-Rich System

Ferrihydrite and gibbsite were supersaturated over the entire pH span in "MIX only" (Fig. 4b). Just as for the BO system, other solid phases would precipitate, lowering the SI and the calculated pH (Fig. 3b). The large discrepancy between SI measured and SI "MIX only" for Zn at high pH illustrates that Zn removal is not merely due to hydroxide precipitation, but also due to smithsonite precipitation and co-precipitation (with Fe, Al). Calculated pH and alkalinities agreed well with measured data when lower SI 0.5 units were used (for ferrihydrite, gibbsite, and zinc hydroxide, respectively, Fig. 3b). Zn hydrolysis (Eq. 7) would contribute to the pH buffering capacity of the Zn system:

$$Zn^{2+} + 2H_2O \leftrightarrow Zn(OH)_2(s) + 2H^+ \quad (7)$$

Mn also precipitates at a pH of 8–9, and could therefore also decrease alkalinity. However, Mn precipitates were not at all dominant in the system.

LB System: Aluminum-Rich System

Ferrihydrite as well as manganite appears to be undersaturated, and gibbsite as well as zinc hydroxide (at high pH) supersaturated when the measured SIs were compared

to the SIs from "MIX only" calculations (Fig. 4c). The Fe levels were low and the contribution from Fe precipitation on pH was minor compared with Al. A reduction of the SI from the "MIX only" calculations by 0.5 units for gibbsite, zinc hydroxide, and smithsonite resulted in a fair agreement between measured and calculated pH and alkalinities (Fig. 3c).

Conclusions

The Fe-dominated BO system is the most classic ARD of the three studied, showing two distinct buffering plateaus due to Fe and Al hydrolysis. In the LG system, Fe was not dominant and was completely removed from solution at pH $\geq$ 4. All mixtures would hence contain Fe precipitates, but no significant buffering from the Fe phases. Instead, Al and Zn (as well as Mg) were the main buffering elements in the less well buffered LG and LB systems. For these systems, with minor Fe precipitates, Zn seems to precipitate as a carbonate at lower pH values (between 6.5 and 7.5) than in the BO system (between 7.5 and 9). Zn would be retained by sorption to the large amount of Fe precipitates already present $\geq$pH 5.5. An additional sink for dissolved Zn could be incorporation into the Mn phase, chalcophanite. Buffering from Mn is negligible in all systems mainly because (1) Mn was not a dominant element in any of the systems, and (2) Mn precipitates at $\approx$pH 6.5 (BO) and 7 (LB and LG), which is when buffering from magnesite precipitation, for example, dominates.

Titration studies of ARD generally do not continue above pH 9 (España et al. 2006; Totsche et al. 2003, 2006) and so the removal of Mg from solution at high pH is not commonly discussed. Mg was found in precipitates after a continuous titration to pH 8.5 (Totsche et al. 2003) and in pH 7 precipitates (España et al. 2006). The solid phase was assessed as coprecipitation between Mg and Al, (as $MgAl(OH)_n$), as well as other solid Al phases with adsorbed Mg. Lee et al. (2002) suggested the formation of insoluble magnesium hydroxide or sorption to other precipitates, but geochemical simulations indicate that magnesium hydroxide formation should not be expected. In the present study, however, Mg precipitation had a large effect on alkalinity (decreasing it in the LG system at pH $\approx$ 8, due to magnesite precipitation), and precipitation of brucite at pH $>$ 10.5 was assumed for all three systems.

Geochemical simulations using PHREEQC, with the MIX keyword, and introduction of proxy phases, can be developed into a method to estimate buffering regions and alkalinity, since these calculations are easily performed. If used correctly, this approach will give a clear picture of the main buffering processes and expected alkalinity production. Analysis of end-members and assessment of other expected solid phases as input in simulations of buffering effects and pH development should be more efficient than performing mixing experiments and titrations.

Acknowledgments This project is part of the Bergskraft program, and access to laboratory facilities as well as administrative support is gratefully acknowledged. Financial support has been received from regional EU funds, from communities in the Bergslagen region, and from Örebro University.

References

Adams JP, Kirst R, Kearns LE, Krekeler MPS (2009) Mn-oxides and sequestration of heavy metals in a suburban catchment basin of the Chesapeake Bay watershed. Environ Geol 58:1269–1280

Allard B, Karlsson S, Lohm U, Sandén P, Bergström S, Brandt M (1987) Environmental impacts of an old mine tailings deposit—hydrochemical and hydrological background. Nord Hydrol 18:279–290

Baas-Becking LGM, Kaplan IR, Moore D (1960) Limits of the natural environment in terms of pH and oxidation-reduction potentials. J Geol 68(3):243–284

Bäckström M, Sartz L (2011) Mixing of acid rock drainage with alkaline leachates—fate and immobilisation of trace elements. Water Air Soil Pollut 222:377–389

Bäckström M, Karlsson U (2006) Ash and sludge covering of mine waste—final report. Benefits and/or risks using ash and sludge for covering of weathered mine waste. Report 960, Thermal Engineering Research Assoc, Sweden (in Swedish, with English summary)

Bäckström M, Sädbom S (2008) Risk assessment of historical mine waste using chemical analysis and ocular mineral/rock classification. In: Proceedings of the 9th international congress for applied mineralogy. Australasian Institute of Mining and Metallurgy, Publ Series 8/2008, p 85–90

Bäckström M, Karlsson S, Ekholm D, Evenhamre P, Skogsjö E (2009) Sediment quality before, during and after remediation of historical mine waste at Bersbo, Sweden. In: Proceedings of the securing the future and 8th ICARD, Skellefteå

Baes CF, Mesmer RE (1976) The hydrolysis of cations. Wiley Interscience, New York City

Baresel C, Destouni G, Gren IM (2006) The influence of metal source uncertainty on cost-effective allocation of mine water pollution abatement in catchments. J Environ Manag 78:138–148

Bigham JM, Schwertmann U, Traina SJ, Winland RL, Wolf M (1996) Schwertmannite and the chemical modeling of iron in acid sulfate waters. Geochim Cosmochim Acta 60:2111–2121

Bowell RJ, Parshley JV (2005) Control of pit-lake water chemistry by secondary minerals, Summer Camp pit, Getchell mine, Nevada. Chem Geol 215:373–385

Burgos WD, Borch T, Troyer LD, Luan F, Larson LN, Brown JF, Lambson J, Shimizu M (2012) Schwertmannite and Fe oxides formed by biological low-pH Fe(II) oxidation versus abiotic neutralization: impact on trace metal sequestration. Geochim Cosmochim Acta 76:29–44

Church CD, Wilkin RT, Alpers CN, Rye RO, McCleskey RB (2007) Microbial sulphate reduction and metal attenuation in pH 4 acid mine water. Geochem Trans 8(10):1–14

Conca JL, Wright J (2006) An apatite II permeable reactive barrier to remediate groundwater containing Zn, Pb and Cd. Appl Geochem 21:1288–1300

Cravotta CA III, Trahan MK (1999) Limestone drains to increase pH and remove dissolved metals from acidic mine drainage. Appl Geochem 14:581–606

Cravotta CA III, Parkhurst DL, Means BP, McKenzie RM, Arthur W (2010) Using the computer program AMDTreat with a PHREEQC titration module to compute caustic quantity, effluent quality, and sludge volume. In: Wolkersdorfer C, Freund A (eds) Mine water and innovative thinking. CBU Press, Sydney, pp 111–114. ISBN 978-1-897009-47-5

Davis A, Eary LE, Helgen S (1999) Assessing the efficacy of lime amendment to geochemically stabilize mine tailings. Environ Sci Technol 33:2626–2632

España JS, Pamo EL, Pastor ES, Andrés JR, Rubí JAM (2006) The removal of dissolved metals by hydroxysulphate precipitates during oxidation and neutralization of acid mine waters, Iberian Pyrite Belt. Aquat Geochem 12:269–298

Gitari MW, Petrik LF, Etchebers O, Key DL, Iwuoha E, Okujeni C (2006) Treatment of acid mine drainage with fly ash: removal of major contaminants and trace elements. J Environ Sci Health A 41:1729–1747

Gitari MW, Petrik LF, Etchebers O, Key DL, Iwuoha E, Okujeni C (2008) Passive neutralization of acid mine drainage by fly ash and its derivates: a column leaching study. Fuel 87:1637–1650

Hayes SM, White SA, Thompson TL, Maier RM, Chorover J (2009) Changes in lead and zinc lability during weathering-induced acidification of desert mine tailings: coupling chemical and micro-scale analyses. Appl Geochem 24:2234–2245

Herbert Jr RB (2006) Seasonal variations in the composition of mine drainage-contaminated groundwater in Dalarna, Sweden. J Geochem Expl 90:197–214

Johansson I (2003) Characterisation of organic materials from incineration residues. PhD thesis, Örebro studies in chemistry 3, Örebro Univ, Örebro, Sweden

Jones WP, Jandik P (1991) Controlled changes of selectivity in the separation of ions by capillary electrophoresis. J Chrom 546:445–458

Karlsson S, Bäckström M (2003) Surface water quality in Bersbo, Sweden – fifteen years after amelioration of sulphidic waste. Proc, Mining and the Environment III, Sudbury, Canada (CD-ROM)

Korshin GV, Chang H-S, Frenkel AI, Ferguson JF (2007) Structural study of the incorporation of heavy metals into solid phase formed during the oxidation of EDTA by permanganate at high pH. Environ Sci Technol 41:2560–2565

Kruse NA, Mackey AL, Bowman JR, Brewster K, Riefler RG (2012) Alkalinity production as an indicator of failure in steel slag leach beds treating acid mine drainage. Environ Earth Sci 67(5):1389–1395

Kwon KD, Refson K, Sposito G (2009) Zinc surface complexes on birnessite: a density functional theory study. Geochim Cosmochim Acta 73:1273–1284

Lee G, Bigham JM, Faure G (2002) Removal of trace metals by coprecipitation with Fe, Al and Mn from natural waters contaminated with acid mine drainage in the Ducktown Mining District, Tennesse. Appl Geochem 17:569–581

Leentvaar J, Rebhun M (1982) Effect of magnesium and calcium precipitation on coagulation–flocculation with lime. Water Res 16:655–662

Lefebvre R, Hockley D, Smolensky J, Gélinas P (2001) Multiphase transfer processes in waste rock piles producing acid mine drainage. 1. Conceptual model and system characterization. J Contam Hydrol 52:137–164

Liu JY, Kalin M (1992) Determination of metal ions in acid mine drainage using a simple titration method. In: Proceedings of the 42nd Canadian chemical engineering conference, Toronto, Canada, p 103–104

Mackie AL, Walsh ME (2012) Bench-scale study of active mine water treatment using cement kiln dust (CKD) as a neutralization agent. Water Res 46:327–334

Moncur MC, Ptacek CJ, Blowes DW, Jambor JL (2006) Spatial variations in water composition at a northern Canadian lake impacted by mine drainage. Appl Geochem 21:1799–1817

Nordstrom DK (1982) The effect of sulfate on aluminum concentrations in natural waters: some stability relations in the system Al_2O_3–SO_3–H_2O at 298 K. Geochim Cosmochim Acta 46:681–692

Parkhurst DL, Appelo CAJ (1999) Useŕs guide to PHREEQC—a computer program for speciation, batch-reaction, one-dimensional transport, and inverse geochemical calculations. USGS WRI Report 99-4259

Pavasars I, Fällman A-M, Allard B, Borén H (1997) Organic substances in leachates from combustion residues. In: Goumans JJJM, Senden GJ, van der Sloot HS (eds) Waste materials in construction: putting theory into practice. Elsevier, Amsterdam, pp 705–714

Pérez-López R, Nieto JM, Álvarez-Valero AM, de Almodóvar GR (2007a) Mineralogy of the hardpan formation processes in the interface between sulfide-rich sludge and fly ash: applications for acid mine drainage mitigation. Am Mineral 92:1966–1977

Pérez-López R, Nieto JM, de Almodóvar GR (2007b) Immobilization of toxic elements in mine residues derived from mining activities in the Iberian Pyrite Belt (SW Spain): laboratory experiments. Appl Geochem 22:1919–1935

Pettersson C, Håkansson K, Karlsson S, Allard B (1993) Metal speciation in a humic surface water system polluted by acidic leachates from a mine deposit in Sweden. Water Res 27:863–871

Pillay P, Barnes DE, van Staden JF (2001) Overcoming interference from hydrolysable cations during the determination of sulphuric acid by titration. Anal Chim Acta 440:45–52

Polat M, Guler E, Akar G, Mordogan H, Ipekoglu U, Cohen H (2002) Neutralization of acid mine drainage by Turkish lignitic fly ashes; role of organic additives in the fixation of toxic elements. J Chem Technol Biotechnol 77:372–376

Romano J, Jandik P, Jones WR, Jackson PE (1991) Optimization of inorganic capillary electrophoresis for the analysis of anionic solutes in real samples. J Chrom 546:411–421

Sartz L (2010) Alkaline amendments for remediation of historic mine sites. PhD thesis, Örebro studies in environmental science 15, Örebro Univ, Örebro, Sweden

Sayilgan E, Kukrer T, Yigit NO, Civelekoglu G, Kitis M (2010) Acidic leaching and precipitation of zinc and manganese from spent battery powders using various reductants. J Hazard Mater 173:137–143

Schindler PW, Stumm W (1987) The surface chemistry of oxides, hydroxides and oxide minerals. In: Stumm W (ed) Aquatic surface chemistry. Wiley, New York City, pp 83–110

Schroth AW, Parnell RA Jr (2005) Trace metal retention through the schwertmannite to goethite transformation as observed in a field setting, Alta Mine, MT. Appl Geochem 20:907–917

Shum M, Lavkulich LM (1999a) Use of sample color to estimate oxidized Fe content in mine waste rock. Environ Geol 37(4):281–289

Shum M, Lavkulich L (1999b) Speciation and solubility relationships of Al, Cu and Fe in solutions associated with sulfuric acid leached mine waste rock. Environ Geol 38(1):59–68

Simmons J, Ziemkiewicz P, Black DC (2002) Use of steel slag leach beds for the treatment of acid mine drainage. Mine Water Environ 21:91–99

Swedish Standards Institute (2002) Water quality—determination of alkalinity—part 2: determination of carbonate alkalinity, ISO Standard 9963-2

Tegengren FR (1924) Sveriges ädlare malmer och bergverk. Swed Geol Surv Ser CA Norstedts Stockh 17:313–329 **(in Swedish)**

Totsche O, Pöthig R, Uhlmann W, Büttcher H, Steinberg CEW (2003) Buffering mechanisms in acidic mining lakes—a model-based analysis. Aquat Geochem 9:343–359

Totsche O, Fyson A, Kalin M, Steinberg CEW (2006) Titration curves—a useful instrument for assessing the buffer systems of acidic mining waters. Environ Sci Pollut Res 13(4):215–224

Valiente M, Diez S, Masana A, Frias C, Muhammed M (1991) Separation of copper and zinc from waste acidic mine effluents of Rio Tinto area. Mine Water Environ 10:17–28

Varesel MT, Gomes CL (2009) Occurrence, properties and pollution potential of environmental minerals in acid mine drainage. Sci Total Environ 407:1135–1152

Wu P, Tang C, Liu C, Zhu L, Pei T, Feng L (2009) Geochemical distribution and removal of As, Fe, Mn and Al in a surface water system affected by acid mine drainage at a coalfield in Southwestern China. Environ Geol 57:1457–1467

Xenidis A, Mylona E, Paspaliaris I (2002) Potential use of lignite fly ash for the control of acid generation from sulphidic wastes. Waste Manag 22:631–641

Yanful EK, Riley MD, Woyshner MR, Duncan J (1993) Construction and monitoring of a composite soil cover on an experimental waste-rock pile near Newcastle, New Brunswick, Canada. Can Geotech J 30:588–599

Yu J-Y, Heo B, Choi J-P, Chang H-W (1999) Apparent solubilities of schwertmannite and ferrihydrite in natural stream waters polluted by mine drainage. Geochim Cosmochim Acta 63(19–20):3407–3416

Zhu M, Legg B, Zhang H, Gilbert B, Ren Y, Banfield JF, Waychunas GA (2012) Early stage formation of iron oxyhydroxides during neutralization of simulated acid mine drainage solutions. Environ Sci Technol 46:8140–8147